



**HAL**  
open science

## Cation redistribution upon dehydration of Na 58 Y faujasite zeolite: a joint neutron diffraction and molecular simulation study

Wilfried Louisfrema, Benjamin Rotenberg, Florence Porcher, Jean-Louis Paillaud, Pascale Massiani, Anne Boutin

### ► To cite this version:

Wilfried Louisfrema, Benjamin Rotenberg, Florence Porcher, Jean-Louis Paillaud, Pascale Massiani, et al.. Cation redistribution upon dehydration of Na 58 Y faujasite zeolite: a joint neutron diffraction and molecular simulation study. *Molecular Simulation*, 2015, 41 (16-17), pp.1371-1378. 10.1080/08927022.2015.1027889 . hal-01284815

**HAL Id: hal-01284815**

**<https://hal.sorbonne-universite.fr/hal-01284815>**

Submitted on 8 Mar 2016

**HAL** is a multi-disciplinary open access archive for the deposit and dissemination of scientific research documents, whether they are published or not. The documents may come from teaching and research institutions in France or abroad, or from public or private research centers.

L'archive ouverte pluridisciplinaire **HAL**, est destinée au dépôt et à la diffusion de documents scientifiques de niveau recherche, publiés ou non, émanant des établissements d'enseignement et de recherche français ou étrangers, des laboratoires publics ou privés.

**Cation redistribution upon dehydration of Na<sub>58</sub>Y faujasite zeolite:  
a joint neutron diffraction and molecular simulation study**

Wilfried Louisfremea<sup>a,b</sup>, Benjamin Rotenberg<sup>b</sup>, Florence Porcher<sup>c,d</sup>, Jean-Louis Paillaud<sup>e</sup>, Pascale Massiani<sup>f</sup>, Anne Boutin<sup>a</sup>

<sup>a</sup> *Ecole Normale Supérieure, PSL Research University, CNRS, UMR PASTEUR, Sorbonne Université, UPMC Univ Paris 06, F-75005 Paris, France*

<sup>b</sup> *Sorbonne Université, UPMC Univ Paris 06, CNRS, UMR PHENIX, F-75005 Paris, France*

<sup>c</sup> *CNRS, CEA, UMR, Laboratoire Léon Brillouin, F-91191 Gif-sur-Yvette Cedex, France*

<sup>d</sup> *Univ Lorraine, CNRS, UMR CRM2, F-54506 Vandœuvre-lès-Nancy, France.*

<sup>e</sup> *Univ Haute-Alsace UHA, CNRS, UMR IS2M, F-68093 Mulhouse, France*

<sup>f</sup> *Sorbonne Université, UPMC Univ Paris 06, CNRS, UMR LRS, F-75005 Paris, France*

Corresponding authors: [anne.boutin@ens.fr](mailto:anne.boutin@ens.fr) & [benjamin.rotenberg@upmc.fr](mailto:benjamin.rotenberg@upmc.fr)

# **Cation redistribution upon dehydration of Na<sub>58</sub>Y faujasite zeolite: a joint neutron diffraction and molecular simulation study**

## **Abstract**

Using neutron scattering and Monte Carlo simulation, we investigate the distribution of cations in Na<sub>58</sub>Y faujasite upon (de)hydration. We introduce a new method for the assignment of cations to specific sites in molecular simulations from their local environment. This allows us to bypass the need of the coordinates of crystallographic sites, which vary as water adsorption induces changes in the zeolite framework structure. While the agreement between experiments and simulation is excellent at high temperature, some differences are observed below 150°C. We show that these differences are due to the presence of water and that temperature itself as well as adsorption-induced deformation of the framework play a less important role. We demonstrate the migration of sodium to sites III upon water adsorption, not observed for other Si:Al ratios.

**Keywords:** Faujasite, cation localization, hydration, Monte Carlo, Neutron diffraction

## **Introduction**

Faujasite-type zeolites have been extensively studied, among other crystalline aluminosilicates, due to their industrial importance in gas adsorption and separation. The location of cations outside the zeolite framework has attracted much attention due its pivotal role in adsorption properties. The precise determination of cation location has thus been the subject of many works, both experimental and theoretical [1]. Extra-framework cations are located in well-defined crystallographic sites [2] but their distribution among these sites is still a subject of fundamental studies. One of the

reasons for the discrepancy between cation location results is the strong sensitivity of cation distribution to experimental conditions (temperature, dehydration conditions, nature and quantity of sorbed molecules ...) [1,3]. The presence of water has been shown to drastically modify the cation location in zeolites and in particular in faujasite zeolite [4,5,6,7,8]. The experimental determination of cation location in hydrated sample is complicated because of partial occupancies affecting low symmetry sites. From the simulation point of view, such a determination suffers from convergence and force field issues. Water adsorption has been previously studied by Monte-Carlo simulation in several sodium faujasites with Si:Al ratio of 1.53, 2.69 and 3 with a unique rigid zeolitic framework and cation redistribution have been evidenced [6].

More recently, a joint experimental and simulation study of cobalt-exchanged X faujasite revealed that the aluminosilicate framework, which exhibits structural deformation upon water adsorption and subsequently cation redistribution, can also affect the cation location [9]. In the present work, we thus undertake a new series of neutron diffraction experiments and molecular simulations to study the cation distribution in a sodium Y faujasite with a Si:Al ratio of 2.3 at various water contents by heating the sample under vacuum. Thanks to the  $^1\text{H}$  incoherent signal in the neutron powder diffraction patterns, the precise water content can be determined together with the cation location and framework structure. We also perform Monte-Carlo simulation to access the cation location under the same conditions as in the experiments, and to study the effects of water loading, temperature and framework structure separately. Section 1 summarizes the experimental and simulation methods. In section 2, we introduce a new methodology to localize cations from their local environment instead of the crystallographic coordinates of the sites. Finally, we present and discuss in Section 3 the agreement between experimental and simulation results.

## 1. Materials and methods

### *Experiments*

The NaY sample, hereafter named Na<sub>58</sub>Y, is a Linde SK-40 zeolite from Union Carbide Corporation. Its unit cell composition, Na<sub>58</sub>Al<sub>58</sub>Si<sub>134</sub> (Si/Al ratio = 2.3), is determined from elemental analysis by wavelength dispersive X-ray fluorescence spectroscopy using a PHILIPS MagiX apparatus.

Neutron powder diffraction experiments are conducted on the two-axis powder diffractometer G4-1 of the LLB-Orphée facility at CEA/Saclay. G4-1 is equipped with a vertically focusing 200 pyrolytic graphite monochromator and a 800-cell multi-detector covering a 80° range in 2θ (Δθ=0.1° between 2 cells), with a nominal wavelength of 2.4226 Å. The evolution of the sample dehydration is followed from room temperature to 400 °C in a furnace under vacuum (P~10<sup>-5</sup> mbar) using an open Vanadium sample holder. The powder neutron diffraction patterns are systematically recorded (8-88°, 15 minutes per scan) all along the treatment. At each step, pressure stabilization is ensured before further temperature increase.

The Rietveld refinements are performed with the GSAS package [10] on the complete pattern via the EXPGUI interface [11].

### *Monte Carlo simulations*

For a better understanding of the microscopic structure of Na<sub>58</sub>Y and its evolution with temperature and water content, we also carry out a series of MC simulations aiming at localizing Na<sup>+</sup> cations and water molecules in different situations corresponding to the experiments described above. Several issues must be addressed. Firstly, the

experimental structure of the zeolite framework, including the lattice parameter, evolves as a function of T and water content. Since MC simulations using standard force fields consider the framework as rigid, it is not possible to simply use a single model simulated under different conditions. Due to this lack of transferability, we rather perform, for each target experimental conditions, simulations using the structure deduced from the experiments (see below). Then, the experimental water content from the diffraction patterns is used to account for experiments at a given temperature. In parallel, we also conduct a set of systematic studies for several experimental structures (labelled in the following by the temperature at which the experiments are performed), as a function of water content. Finally, the convergence of the MC simulations must be carefully monitored, and special care is taken to ensure that the simulations are not trapped in metastable states, as explained below.

All interactions between framework atoms, cations and water molecules are described by pairwise additive potentials of the Coulomb (electrostatic interactions) and Lennard-Jones (repulsion and dispersion) forms. The parameters are taken from Jaramillo et al. [12] for the zeolite framework (in particular, Si and Al atoms are described as "T atoms" carrying identical charges) and from Dang et al. [13] for Na<sup>+</sup> cations, together with the TIP4P water model of water [14]. This force field was successfully used in previous studies of water adsorption in Y and X zeolites [4,5,6,15,16]. Periodic boundary conditions are used, electrostatic interactions are computed using Ewald summation and a cut-off equal to half the box length is used to compute Lennard-Jones interactions.

For each system, a random initial configuration is generated for the cations. Water is then inserted by Grand Canonical Monte Carlo (GCMC) simulation, while keeping the ions fixed, until the target water content is reached. Subsequent simulations

are performed in the canonical ensemble for  $6 \cdot 10^7$  MC steps. The sampling of configuration space is enhanced by using "jump moves", *i.e.* large amplitude trial displacements for the cations, and by simulating the system at 700 K. While this does not correspond to the target temperature, we observed that it provides in the cases under consideration the same results as parallel tempering [5,17] at a much lower computational cost (only one temperature is used, instead of the 14 replicas for our parallel tempering simulations). In particular, we have checked that this procedure allows us to obtain reproducible results starting from uncorrelated initial conditions, and to overcome possible free energy barriers separating metastable cation distributions, which may result in hysteresis in the hydration/dehydration processes.

## **2. A new method for cation localization in molecular simulation**

### *From crystallographic sites*

Cations in zeolites are usually localized on specific sites, which depend on the aluminosilicate framework. The standard definition of these sites follows from their coordinates in the crystal unit cell, which have to be determined experimentally. **Figure 1** shows a schematic representation of the faujasite structure with the location of the four types of cationic sites widely documented in the literature [1]. For the specific case of Faujasite, sites I, I' and II lie along the [1,1,1]-axis, situated respectively at the centre of the hexagonal prism (site I), inside the sodalite cage (site I'), and inside the supercages facing the 6-membered ring window of the sodalite cage (site II). Sites III are located inside the supercages facing 4-membered rings of the aluminosilicate framework, between two other 4-membered rings. In some cases, an additional fifth site type (II') is

defined: It corresponds to a shift of site II within the sodalite cage. The total numbers of sites I, I', II, II' and III are 16, 32, 32, 32 and 48 per unit cell, respectively.

The standard method for assigning a cation to a specific site is then based on its distance to all possible crystallographic sites in the unit cell. More specifically, this is achieved by testing whether the distance to all sites of one type is smaller than a prescribed cut-off, and if no such site is found the process is continued with the next type of site. In practice, sites are tested in the order I, I', II, II' and III, and the following cut-offs are used accordingly: 1.09, 2.8, 2.0, 2.0 and 2.5 Å. **Figure 2** illustrates the regions corresponding to each site type.

### ***From the local environment***

The standard method requires the knowledge of the coordinates of the crystallographic sites, which change as the system evolves with temperature or water content. In addition, for a flexible framework the instantaneous configuration differs from the average one, so that the definition of crystallographic sites may become problematic. Here we introduce a new localization method for the analysis of molecular simulations, based on the local environment of the cations for each configuration.

Our approach follows from the observation that four different oxygen types may be distinguished in the zeolite framework, as illustrated in **Figure 3**, and that cations localized in different crystallographic sites are coordinated by different numbers of each oxygen type. We introduce a set of criteria to assign each cation to a given type of crystallographic site, according to the coordination

numbers by each oxygen type, from O1 to O4 (see **Figure 3**). More specifically, O1 bridging Si or Al atoms form the edges of the lateral faces of hexagonal prisms. The edges of the other two faces of these hexagonal prisms, which connect them to the neighbouring cub-octahedral sodalite cages, are occupied alternatively by O3 and O4. O3 also belong to the square faces of the sodalite cages, while O4 also belong to the hexagonal window between the sodalite and supercages. Finally, O2 are located on the shared edges between the square faces and sodalite-supercage hexagonal windows.

The coordination numbers are computed for a common value of cut-off radius  $R_{\text{cut}} = 3.7 \text{ \AA}$ , which was set in accordance with the following criteria:

- Site I: Presence of O1, absence of O2, and total coordination number (by O1, O2, O3 and O4) smaller than or equal to 6,
- Site I': Absence of O1 and O2,
- Site II: Absence of O1 and O4,
- Site II': Absence of O1, presence of O2 and more O4 than O3,
- Site III: Absence of O3,

where the absence of a given oxygen type is defined with a tolerance of 1 atom (i.e. 0 or 1 atom of this type). This set of simple rules and the corresponding cut-off distance was designed by trial and error, so as to obtain identical assignment of the sites for each cation (and not only the average distribution among sites) as with the standard definition, for random cation configurations, including some that are not relevant to the present case (as shown below, some sites are absent for  $\text{Na}_{58}\text{Y}$ ). It is worth mentioning that the cation distribution resulting from these criteria is not sensitive to the precise

value of the cut-off in the range 3.4 – 3.7 Å and that, as with the standard method, some cations may in some cases not be assigned to any type of site.

As an illustration of the validity of the method, **Table 1** compares the average distribution of cations obtained with both localization methods for the specific case of the structure at 20°C and 15 water molecules per unit cell. The agreement between both approaches is excellent and results reported below correspond to the new method introduced in the present work. Only a few exceptions are observed, in general with cations at the boundaries of regions defined by the standard method. This new method is versatile and will be useful for the analysis of simulations with flexible frameworks, as required in particular in the presence of multivalent cations. As a first step in this direction, we have tested it for configurations from a molecular dynamics simulation of a flexible NaY and found that it provides for each cation a localization that is consistent with visual inspection (not shown). While the present strategy based on the local environment is very general, we note as a caveat that the criteria (and corresponding cut-off) listed above are appropriate for Faujasite-type zeolites but should be adapted for other zeolite frameworks.

### **3. Results: cation localization vs water content and temperature**

#### *Experimental results*

The evolution of the neutron powder patterns of Na<sub>58</sub>Y during heating to increasing temperatures under vacuum is shown on **Figure 4**. All patterns are characteristic of a highly crystalline FAU structure. As illustrated in the inset of the figure, the position of the 111 diffraction line slightly shifts toward smaller angles with increasing

temperature. This change is due to the lattice expansion upon heating [18], with lattice parameters ranging from 24.679(1) Å at 20°C to 24.834(1) Å at 400°C (see **Table 2**).

More interestingly, the background signal, due to incoherent scattering by hydrogen atoms from water molecules present in the sample, decreases in intensity upon dehydration. Its variation is quantitatively illustrated in **Figure 5** where each point is the mean value of the 30 data points collected at each temperature for  $2\theta$  between 12 and 15°, a region of the powder patterns free of diffraction peaks. Thus, it is possible to follow in real time the dehydration process and to evaluate at each temperature the remaining amount of water in the sample. The water contents in the various samples obtained by neutron diffraction are summarized in **Table 2**. At the start of the experiment (*i.e.* after pumping at room temperature), the initial water content was found to be 8 wt. %, or ~63 water molecules per unit cell, *i.e.* on average approximately 1 molecule per cation. Next, the data suggest that the zeolite dehydration in vacuum takes place regularly during heating between RT and 150°C and is almost complete at 200°C. The residual amount of water at 150°C is 0.8 wt. %, *i.e.* about 5 water molecules per unit cell.

Using Rietveld refinements, we evaluate the structural evolutions with dehydration, especially the changes in the cation distribution. In agreement with literature data referred to in the experimental methods section, four distinct crystallographic extra framework cationic sites are found and their positions are consistent with published studies on faujasite with similar Si/Al ratios [1]. **Figure 6** presents the evolution of site occupancies as a function of temperature. After evacuation at room temperature, sites III are predominantly occupied. During the successive heating steps from RT until 150°C, a continuous migration of sodium cations from predominantly sites III toward sites II occurs. At this temperature, *i.e.* after an almost

complete removal of the water molecules, the site distribution stabilizes with a full occupancy of site II. Thereafter, only a slight variation of the interatomic distances is observed upon further heating.

This distribution in the dry samples is essentially controlled by inter-ionic repulsion. Sites II are all occupied, all sites II' are empty and only a few cations are observed in sites III. The remaining cations are distributed between I and I' sites: since there are only 16 I sites per unit cell, the addition of the ~10 remaining cations (neglecting the ones in III sites) displaces cations from I to I' resulting in pairs of I' sites (see **Figure 2**). Consequently the number of cations in sites I decreases to ~6 and that of I' increases to ~18.

The structure analysis of the initial sample after evacuation at room temperature allows us to localize the main part of the water molecules in this partially hydrated faujasite. At this stage, about 8 wt. % of water remains in the pores, as already indicated above. This corresponds to ~63 H<sub>2</sub>O molecules per unit cell. From Rietveld analysis, about 50 of these can be located and are found to be distributed over 3 different crystallographic sites, as illustrated in **Figure 7**. Molecules Ow1 are positioned inside the sodalite cage and are coordinated to cations NaI', while Ow2 and Ow3 sit in the supercages, with Ow2 coordinating both NaII and NaIII, and Ow3 being only connected to NaIII. The observed inter atomic distances between oxygen atoms and cations lie between 2.42 and 2.83 Å in agreement with former crystallographic studies [1].

Changes in the cation distribution at lower temperatures are mainly due to water adsorption. Temperature-induced deformation (as will be discussed below) as well as temperature itself at fixed water content play a less important role. The observed migration of Na<sup>+</sup> cations from sites II to III upon decreasing the temperature had not

been reported previously for Na<sub>58</sub>Y faujasite, but is consistent with the result of Kirschhock et al. for a different Si/Al ratio at low relative humidity [19,20].

### ***Simulation results***

**Figure 8** reports the cation distribution in Na<sub>58</sub>Y as a function of water content. The simulations are performed using rigid frameworks with the experimental structure obtained at each temperature and water contents in the range 0-200 molecules per unit cell. We first note that the effect of the framework structure is rather limited for the range of experimental deformations observed in the present case. In addition, the cation distribution for the dry Na<sub>58</sub>Y ( $N_{\text{water}}=0$ ) is in good agreement with the experimental result. As the water content increases, sites II' remain empty and sites II remain practically all occupied. We also observe an increase in the number of sites III, even though much less pronounced than in the experiments. In the range of experimental water contents, *i.e.* less than ~65 water molecules per unit cell, the population of sites I' decreases while that of sites I increases, and opposite trends are observed for larger water contents. The overall balance between sites suggested by simulation is thus a displacement from sites I and I' to sites III as the water content increases in the experimental range.

With molecular simulations, we can further examine how these changes in the cation distribution correlate with the water localization. Water adsorption essentially takes place in two distinct environments: sodalite cages and supercages. The fraction of molecules in sodalite cages decreases from ~25% at very low water content to ~9% for ~65 water molecules and beyond. This initial preferential adsorption in sodalite cages is associated with the displacement of cations from sites I' (sodalite cages) to sites I

(hexagonal prisms) and III (supercages). Upon further water adsorption, beyond the experimental range, crowding of the sodalite cages by water molecules is likely at the origin of the reverse migration from I' to I sites.

Simulations using the same force field have been reported for other Si:Al ratios [6], corresponding to unit cells with 48, 52 and 76 cations. In dehydrated Na<sub>48</sub>Y, sites I and II are present; upon hydration the migration from sites I to I' correlates with the adsorption of water in sodalite cages. At maximal water loading one reaches 16 sites I' and 32 water molecules in sodalite cages. With Na<sub>52</sub>Y, some sites I' are observed even in the dry state and migration from sites I to I' upon adsorption results in the same final occupancy of I' and water in sodalite cages. Finally, in dehydrated Na<sub>76</sub>X all sites I' are occupied, while all sites I are empty; upon hydration one observes the migration from I' to I. Therefore, the present case of Na<sub>58</sub>Y displays an unusual behaviour, with the migration from I' not only to I but also to sites III. Such sites were not observed for larger Si:Al ratios, and are always occupied for smaller Si:Al ratios.

### ***Discussion***

Compared to the systematic simulation results as a function of water content of the previous section, the experimental results as a function of temperature suggest a more pronounced population of sites III and, more importantly, that these sites are populated at the expense of sites II instead of sites I and I'. Here we push the comparison further by performing simulations more directly comparable to the experiments. For each temperature, we perform simulations with the experimental structure, using the experimental water content (see **Table 2**).

Results are summarized in **Figure 9**. The agreement between simulation and

experiments is excellent for temperatures above 150°C at which the water content is very low. For temperatures below 100°C, the main difference is the origin of the cations in sites III (and their number): sites I/I' in simulations instead of sites II in experiments. One possible source of discrepancy may be the high temperature used for the simulations in these cases to ensure convergence of the results. However, as mentioned above, we have checked for a number of comparable systems that the same results are obtained using the computationally more expensive parallel tempering method.

Another possible source of discrepancy is the force field used to describe the microscopic interactions. In particular, it is essential to correctly capture the competition between ion-solvent and ion-framework interactions [21,22]. As a crude test of the force field used in the present study, we artificially increase the ion-water interaction by multiplying the corresponding Lennard-Jones interaction strength by a factor of 100. Simulations are performed in the 20°C experimental structure for two water contents, namely 63 and 123 water molecules per unit cell, at a temperature of 700K to ensure good convergence. Results are summarized in **Table 3**. One observes a better agreement with experiments, including a large increase in the number of sites III and a pronounced depopulation of sites II, as well as the virtual absence of sites I. Some differences still remain, such as the too large number of sites I' (and II'), or the too small number of sites III. While this ad hoc modification of the model is not able to reproduce the experimental results quantitatively, it clearly suggests that changing the balance between ion-water and ion-framework interactions is a promising perspective for the design of more reliable force fields.

Finally, the use of T atoms to model without distinguishing Si and Al atoms may also contribute to the differences observed with experiments. As such a distinction is not possible experimentally (the Al location has no long range order), simulations with

distinct Si and Al atoms would require an averaging of all properties over several distribution of these species inside the crystalline framework. The cation localization should depend on the specific position of Si and Al. In the case of Faujasite zeolites, we have shown that subsequent averaging over their microscopic distribution results in sodium cation distributions in good agreement with the one predicted with T atoms [23].

## **Conclusion**

Using an innovative neutron scattering approach, we have described in detail the distribution of cations in  $\text{Na}_{58}\text{Y}$  faujasite upon (de)hydration and demonstrated in particular the migration of sodium from sites II to III upon water adsorption. In order to investigate this migration from a molecular perspective, we also performed Monte Carlo simulations. To that end, we used a force field from the literature and the structure determined by neutron diffraction for each experimental condition. We introduced a new localization procedure, allowing for the assignment of each cation to a specific type of site from its local environment (characterized by different types of framework oxygen atoms). This new procedure does not require the knowledge of the crystallographic coordinates of the sites and is particularly well suited to account for flexible frameworks (or as in the present case, several rigid frameworks).

While in quantitative agreement with experiments for high temperatures, when the water content is low, some important differences are observed for temperatures lower than  $100^\circ\text{C}$ , in the presence of adsorbed water. In particular the simulations conclude to a migration from sites I' to III. Simulations using a modified force field with increased cation-water interactions provide results in better agreement with the

experiments. Overall, the present study suggests that the development of more accurate force fields, better accounting for the balance between ion-water and ion-framework interactions as well as for framework flexibility, is highly desirable.

### **Acknowledgements**

WL acknowledges financial support from Région Ile-de-France via the DIM OXYMORE. The authors acknowledge the support of Laboratoire Léon Brillouin at CEA/Saclay for neutron beam time (proposal 11299) and the help of F. Damay and G. André for the experiments on G4.1.

## References

- [1] Frising T, Leflaive P. Extraframework cation distributions in X and Y faujasite zeolites: A review. *Microporous and Mesoporous Materials* 2008;114:27–63.
- [2] Mortier WJ, Van den Bossche E, Uytterhoeven JB. Influence of the temperature and water adsorption on the cation location in Na-Y zeolites. *Zeolites* 1984;4(1):41-44.
- [3] Rubio JA, Soria J, Cano FH. Influence of the dehydration pretreatment on the cation location in NaY zeolite. *J. Colloid Interf. Sci.* 1980;73(2):312-323.
- [4] Beauvais C, Boutin A, Fuchs AH. A Numerical Evidence for Nonframework Cation Redistribution Upon Water Adsorption in Faujasite Zeolite. *ChemPhysChem* 2004;11:1791-1793.
- [5] Beauvais C, Guerrault X, Coudert FX, Boutin A, Fuchs AH. Distribution of Sodium Cations in Faujasite-Type Zeolite: A Canonical Parallel Tempering Simulation Study. *J. Phys. Chem. B* 2004;108(1):399-404.
- [6] Di Lella A, Desbiens N, Boutin A, Demachy I, Ungerer P, Bellat JP, Fuchs AH. Molecular simulation studies of water physisorption in zeolites. *Phys. Chem. Chem. Phys.* 2006;8(46):5396-5406.
- [7] Abrioux C, Coasne B, Maurin G, Henn F, Boutin A, Di Lella A, Nieto-Draghi C, Fuchs AH. A molecular simulation study of the distribution of cation in zeolites. *Adsorption* 2008;14: 743–754.
- [8] Marti J, Soria J, Cano FH. Cation Location in Hydrated NaY Zeolites. *J. Colloid Interf. Sci.* 1977;60(1):82-86.
- [9] Jeffroy M, Borissenko E, Di Lella A, Boutin A, Porcher F, Souhassou M, Lecomte C, Fuchs AH. Evidence of a framework induced cation redistribution upon water adsorption in NaCoX faujasite zeolite. A joint experimental and simulation study. *Micro. Meso. Mat.* 2011;138:45-50
- [10] Larson AC, Von Dreele RB. General Structure Analysis System (GSAS), Los Alamos National Laboratory Report LAUR 86-748 (2004).
- [11] Toby B. EXPGUI, a Graphical User Interface for GSAS. *J. Appl. Crystallogr.*, 2001;34:210.
- [12] Jaramillo E, Auerbach SM. New Force Field for Na Cations in Faujasite-Type Zeolites. *J. Phys. Chem. B* 1999;103(44):9589-9594.
- [13] Dang LX. Mechanism and Thermodynamics of Ion Selectivity in Aqueous Solutions of 18-Crown-6 Ether: A Molecular Dynamics Study. *J. Am. Chem. Soc.* 1995;117: 6954-6960.

- [14] Jorgensen WL, Chandrasekhar J, Madura JD, Impey RW, Klein ML. Comparison of simple potential functions for simulating liquid water. *J. Chem. Phys.* 1983;79(2):926-935.
- [15] Buttefey S, Boutin A, Mellot-Draznieks C, Fuchs AH. A simple model for predicting the Na<sup>+</sup> distribution in anhydrous NaY and NaX zeolites. *J Phys Chem B* 2001;105:9569-9575
- [16] Buttefey S, Boutin A, Fuchs AH. Cation distribution in faujasite-type zeolites : A test of semi-empirical force fields for Na cations. *Molecular Simulation* 2002;28:1049-1062
- [17] Falcioni M, Deem MW. A biased Monte Carlo scheme for zeolite structure solution. *J Chem Phys* 1999;110:1754-1766
- [18] Noack M, Schneider M, Dittmar A, Georgi G, Caro J. The change of the unit cell dimension of different zeolite types by heating and its influence on supported membrane layers. *Microporous and Mesoporous Materials* 2009;117:10–21.
- [19] Kischhock CEA, Hunger B, Martens J, Jacobs PA. Localization of Residual Water in Alkali-Metal Cation-Exchanged X and Y Type Zeolites. *J. Phys. Chem. B* 1999;104(3):439-448.
- [20] Verhulst HAM, Welters WJJ, Vorbeck G, Van de Ven LJM, De Beer VHJ, Van Santen RA, De Haan JW. A new assignment of the signals in <sup>23</sup>Na DOR NMR to sodium sites in dehydrated NaY zeolite. *J Phys Chem* 1994;98:7056-7062
- [21] Rotenberg B, Morel JP, Marry V, Turq P, Morel-Desrosiers N. On the driving force of cation exchange in clays: Insights from combined microcalorimetry experiments and molecular simulation. *Geochim. Cosmochim. Acta* 2009;73(14):4034-4044.
- [22] Jeffroy, M, Boutin A, Fuchs AH. Understanding the Equilibrium Ion Exchange Properties in Faujasite Zeolite from Monte Carlo Simulations. *J. Phys. Chem. B* 2011;115:15059-15066.
- [23] Jeffroy, M. Molecular simulation of cationic zeolites properties : thermodynamic and structural properties PhD Thesis (2010), Université Paris Sud, Orsay, France. <https://tel.archives-ouvertes.fr/tel-00517043>.

**Table 1** Comparison of the cation distribution determined in Na<sub>58</sub>Y from the coordinates of the crystallographic sites (standard method) and from the cation local environment (new method), for the experimental structure at 20°C with 15 water molecules per unit cell. Cations that cannot be assigned to any site are labelled NL (not localized).

<b>Method</b>	<b>I</b>	<b>I'</b>	<b>II</b>	<b>II'</b>	<b>III</b>	<b>NL</b>
Coordinates	8.8±0.4	14.2±0.5	31.8±0.3	0	3.1±0.4	0
Environment	8.8±0.4	14.4±0.4	31.7±0.4	0	2.8±0.5	0.4±0.5

**Table 2** Experimental lattice parameter  $a$  ( $\pm 0.001$  Å) and water content  $N_w$  (number of molecules per unit cell,  $\pm 1.5$ ) as a function of temperature. The fixed number of molecules used in simulations for comparison with experiments is also indicated.

<b>Temperature</b>	<b>20°C</b>	<b>80°C</b>	<b>100°C</b>	<b>150°C</b>	<b>200°C</b>	<b>250°C</b>	<b>300°C</b>	<b>400°C</b>
$a$ (Å)	24.679	24.690	24.745	24.804	24.832	24.839	24.837	24.834
$N_w$ (exp)	61.6	34.8	19.0	5.8	1.5	0	0	0
$N_w$ (sim)	63	35	19	6	1	0	0	0

**Table 3** Cation distribution in Na<sub>58</sub>Y with a modified force field with Lennard-Jones interactions between cations and water increased by a factor of 100. Simulations are performed for the experimental structure at 20°C.

<b>Water / u.c.</b>	<b>I</b>	<b>I'</b>	<b>II</b>	<b>II'</b>	<b>III</b>	<b>NL</b>
63	0.0±0.1	25.7±0.5	9.6±0.5	2.3±0.6	18.0±0.5	2.4±0.5
123	0.0±0.1	18.4±0.7	10.9±1.5	4.9±0.5	21.7±1.5	2.1±1.2

**Figure 1** Schematic representation of cationic sites I, I', II, II' and III in the pores of the faujasite structure.

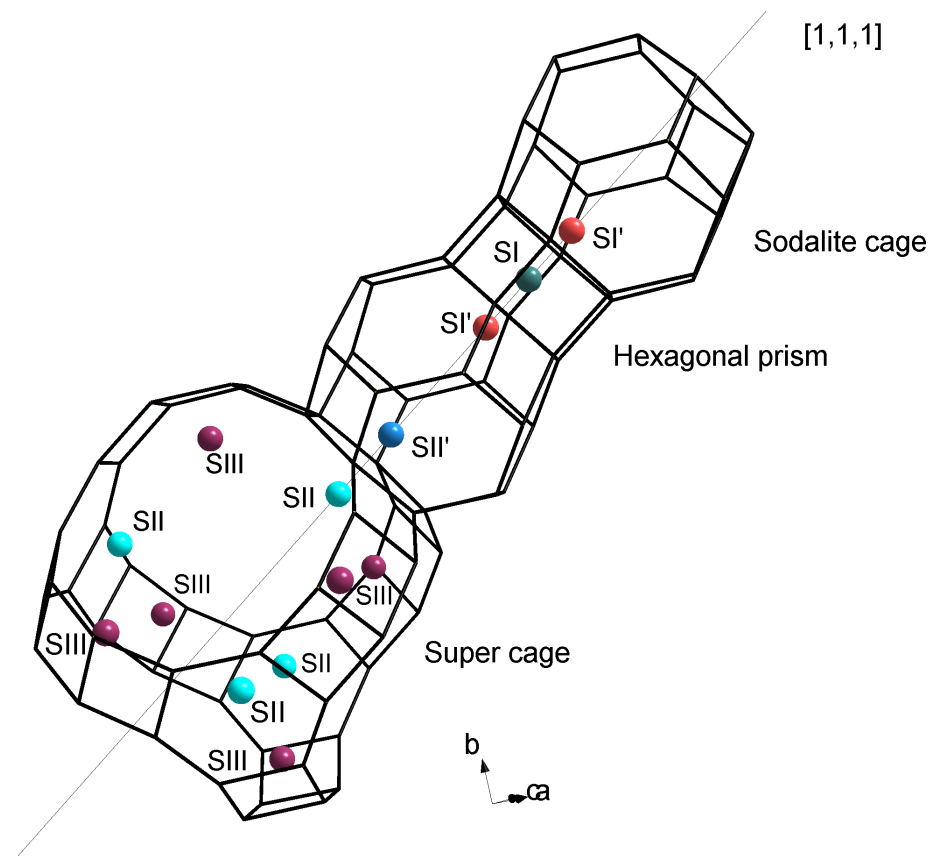


**Figure 2** Definition of the cationic sites from crystallographic coordinates. The radius of the sphere indicates the cut-off distance used to assign each cation to a specific site. Five site types are defined: I (dark blue), I' (cyan), II (purple), II' (brown) and III (green). Framework atoms are indicated in red (O) and yellow (Si and Al). Only a few sites are shown for clarity.

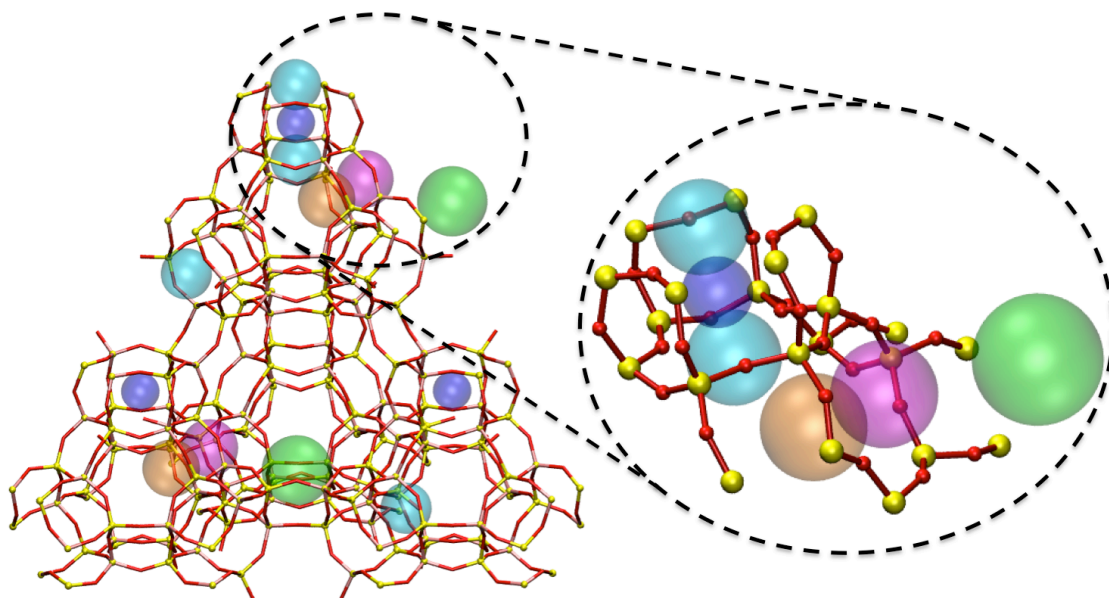


**Figure 3** Definition of the different types of oxygen used to characterize the local environment of each cation and assign them to crystallographic sites: O1 (red), O2 (blue), O3 (orange) and O4 (black). Si and Al atoms are shown in yellow.

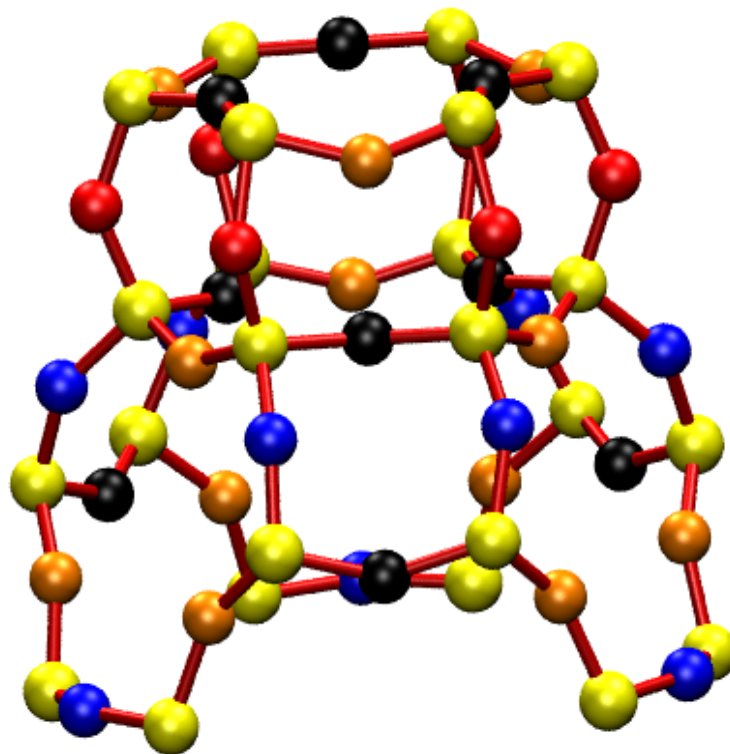


**Figure 4** Powder neutron diffraction patterns of  $\text{Na}_{58}\text{Y}$  as collected on the G4-1 diffractometer at LLB, for temperatures between 20 and 400°C. The inset shows the profile evolution of the 111 diffraction line.

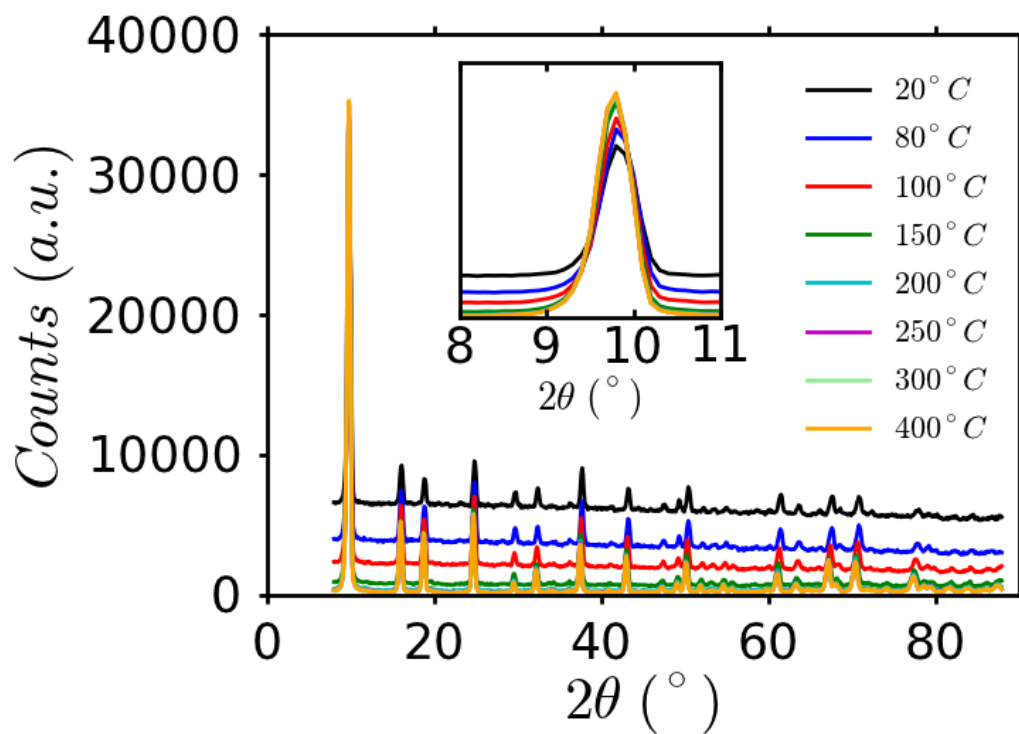


**Figure 5** Evolution of the incoherent signal intensity as a function of temperature. Standard deviations are smaller than the symbols.

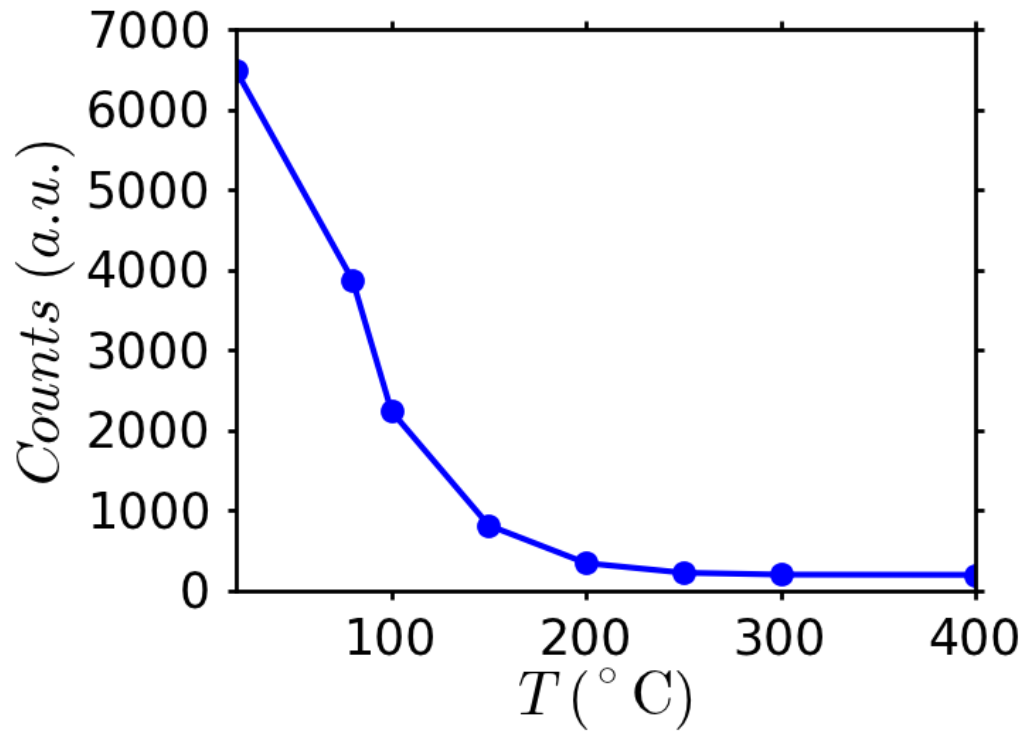


**Figure 6** Number of cations per unit cell in each type of crystallographic site (I, I', II, II' and III) as a function of temperature, as obtained from neutron diffraction. The total numbers of sites per unit cell are 16, 32, 32, 32 and 48 per unit cell, respectively.

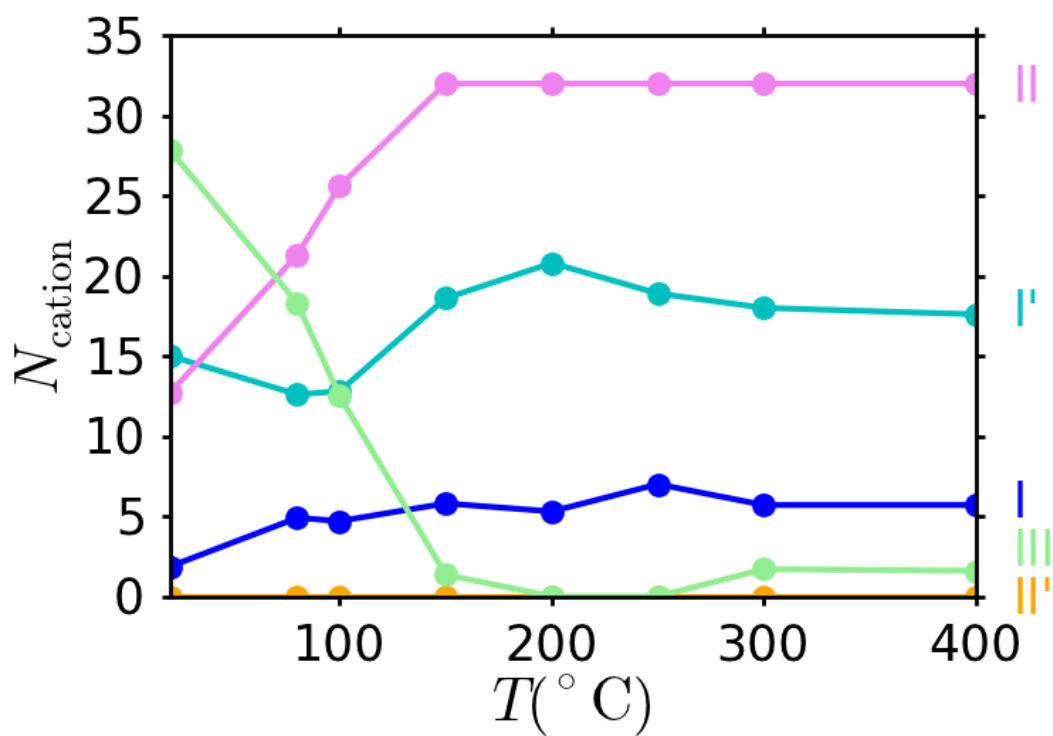


**Figure 7** Perspective view of partially hydrated  $\text{Na}_{58}\text{Y}$  structure showing the sodium coordination to framework oxygen atoms and water molecules. Only one cation per crystallographic site is shown for clarity.

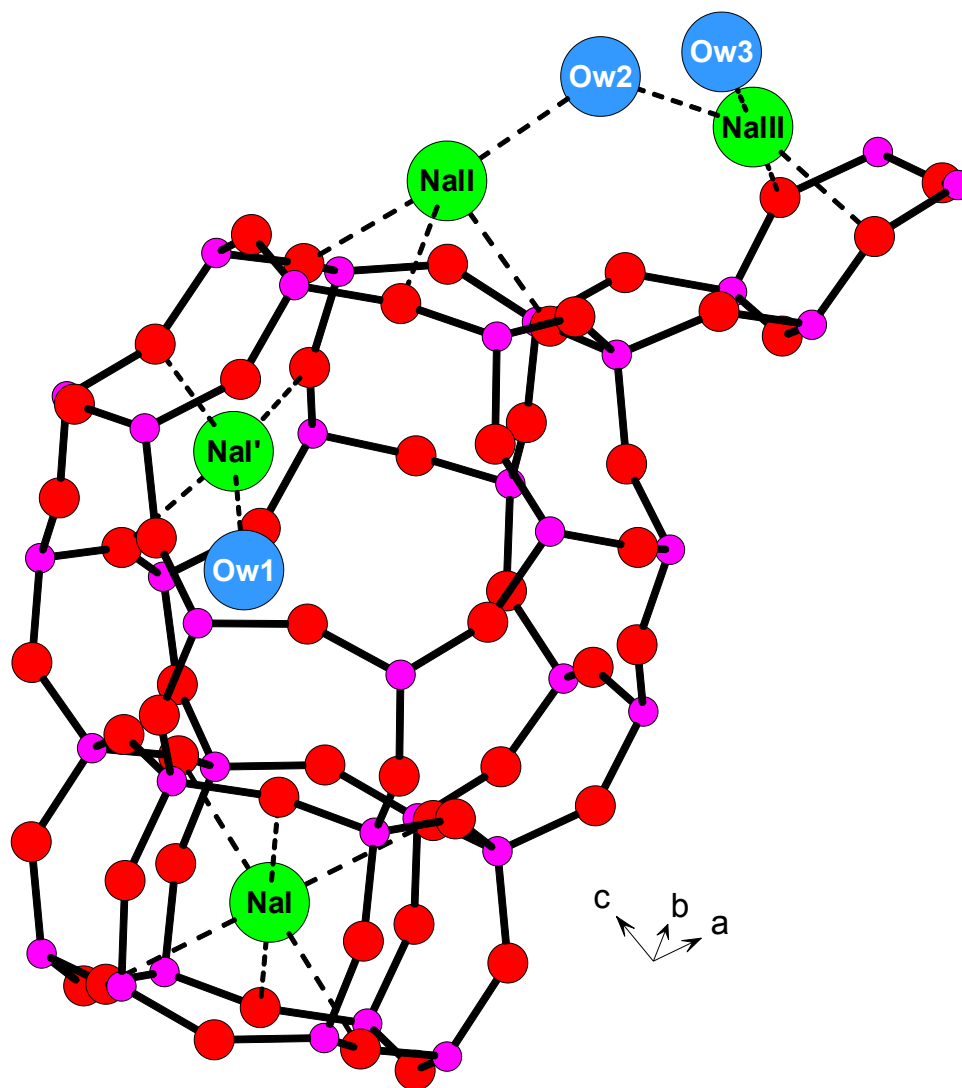


**Figure 8** Number of cations per unit cell in each type of crystallographic site (I, I', II, II' and III) as a function of the water content (number of water molecules per unit cell), as obtained from Monte Carlo simulation. The total numbers of sites per unit cell are 16, 32, 32, 32 and 48 per unit cell, respectively. Temperatures refer to the experimentally determined structure used in the simulations with rigid frameworks (see text for details).

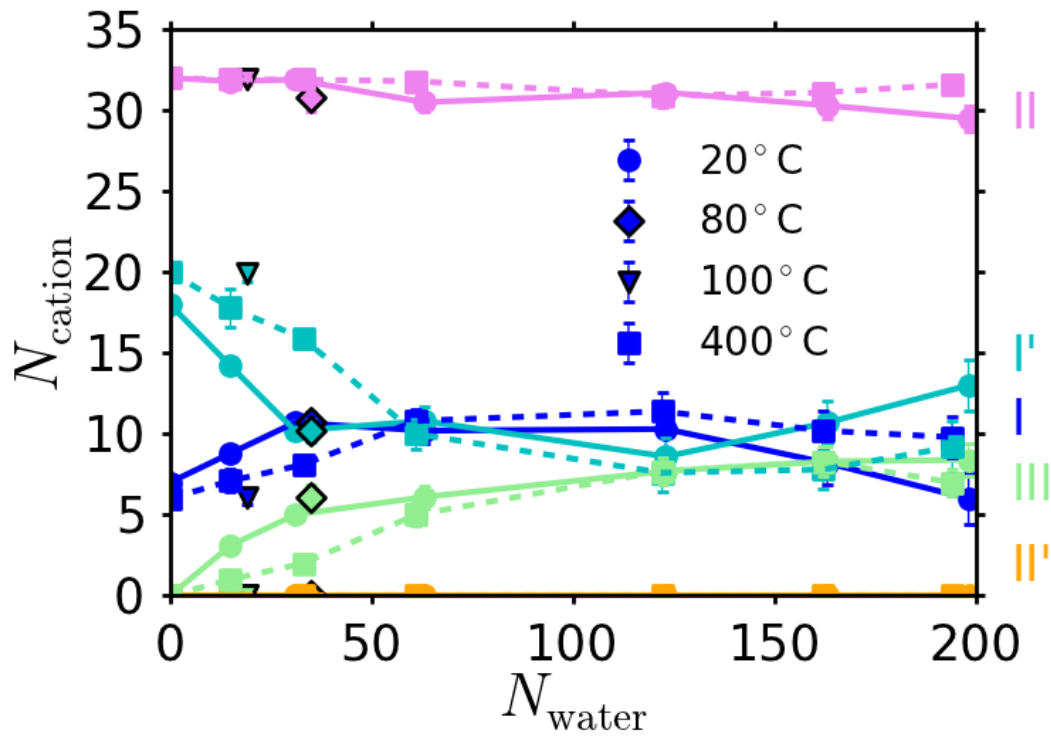


**Figure 9** Number of cations per unit cell in each type of crystallographic site (I, I', II, II' and III) as a function of temperature. Experimental data (same as **Figure 6**) are compared to Monte Carlo simulations with the experimental structure and the experimental water content (see **Table 2**). The total numbers of sites per unit cell are 16, 32, 32, 32 and 48 per unit cell, respectively.

